



THE ROLE OF REFRACTORY ELEMENTS IN ADVANCED ALLOYS AND CERAMICS FOR EXTREME ENVIRONMENTS

Vacuum Brazing of NIMONIC 105 Superalloy Using W-Rich BNi-10 and Conventional BNi-2 Fillers

MOHAMMAD AMMAR MOFID ^{1,3} REZA BARAZANDEH,¹
and MOSTAFA JAFARZADEGAN²

1.—Department of Petroleum, Mining and Material Engineering, Faculty of Civil and Earth Resources Engineering, Central Tehran Branch, Islamic Azad University, Tehran, Iran. 2.—Faculty of Engineering, Imam Khomeini International University (IKIU), Qazvin 3414896818, Iran. 3.—e-mail: moh.ammar_mofid@iauctb.ac.ir

Two different filler metals were used for vacuum brazing of NIMONIC 105 similar joints. At first, the specimen was brazed using BNi-2 as filler. The optimized parameters were brazing time and temperature of 7 min and 1200°C, respectively. Then, the innovative approach of adding tungsten to the braze filler was adopted to improve the metallurgical properties of the joints. The formation of intermetallic and eutectic phases was investigated by back-scattered electron (BSE) imaging, energy dispersive X-ray spectroscopy (EDS), X-ray diffraction (XRD), and hardness testing. The investigation confirmed that, unlike the bulky brittle phases (SiCr₃, Ni₂B, Cr₂B, and NiSi), and network or eutectic phases found in the specimen brazed using BNi-2 as filler, a W-rich filler (BNi-10) creates fine precipitates (CrSi₂, Cr₂B) that have minimal impact on the properties of the joint. Microhardness evaluation indicated that using the BNi-10 filler resulted in more uniform hardness profiles across the joint. The shear strength of brazed joints increased significantly from 81.8 MPa to 88.1 MPa with the addition of tungsten. Lack of Ni₂B and NiSi formation resulted in a high ductility of 17.1% in the specimen brazed via BNi-10 when compared with 10.95% in the specimen brazed via BNi-2.

INTRODUCTION

Nickel (Ni) and Ni-base alloys are widely used in the aeronautics, space, nuclear, chemical, and petrochemical industries for their high corrosion resistance and high strength at elevated temperatures.^{1,2} NIMONIC alloy 105 (W. Nr. 2.4634) is a wrought nickel-cobalt-chromium-base alloy strengthened by additions of molybdenum, aluminum, and titanium. The alloy is appropriate for service temperatures up to 950°C and has the advantage of high strength of age-hardened nickel-base alloys along with good creep resistance. The main application of this alloy is in gas turbine blades, discs, bolts, and fasteners.³ To realize the benefits of joining these parts, the development of reliable joints is required.⁴ Regarding the unique

advantages of wide-gap brazing over other joining processes, this is a feasible approach to join gas turbine components.^{5–8} A vacuum chamber or inert atmosphere is required to perform the process. In such a process, the gap should be wider than 500 μm. According to the literature, the formation of eutectic and brittle intermetallic phases is inevitable. This problem arises from the nature of the brazing process and results in deterioration of the strength of the joint.⁸ These brittle phases would not only have a detrimental effect on the high-temperature performance of the alloy but also make it prone to oxidation or selective corrosion.^{5,8,9} Controlling the joining variables will not properly avoid the formation of intermetallic phases.^{10–19}

The most common filler for brazing Ni superalloys is BNi-2 braze alloys that contain boron and silicon as melting point depressants (MPDs). The BNi filler metals are commonly used on stainless steels for oxidation resistance at temperatures up to 980–1095°C.² However, the problem is that this filler

(Received December 1, 2022; accepted May 30, 2023; published online June 21, 2023)

develops a brittle eutectic constituent that is the source for crack initiation and propagation.^{20,21} One approach to overcoming or at least moderating the unfavorable impact of such eutectic and intermetallic phases is by applying subsequent diffusion treatment to enhance the diffusion of B (and Si) and to reduce the size of intermetallic compounds (IMCs). However, investigations have shown that even homogenization treatment after the brazing process could not effectively dissolve undesirable phases.²² In addition to time and energy-consuming post-braze heat treatment, another approach can be employed to reduce the size of brittle phases. In one particular method, composite fillers, which are prepared by introducing tiny ceramic particles or fibers into traditional active brazing fillers, are utilized. In this approach, atomic diffusion is retarded and, as a result, the formation of brittle intermetallics can be controlled.²³ Much research has been devoted to overcoming or at least moderating the unfavorable impact of such brittle phases by introducing silicon nanoparticles, graphene, ZrO₂ nanoparticles, TiO₂ nanoparticles, and tungsten powder into the brazing filler.^{23–25} Liu et al. concluded that adding graphene significantly improved the shear strength of GH99 superalloy brazed joints. They claimed that graphene effectively retarded atomic diffusion and controlled the formation of brittle boride precipitates.²³ García et al. used silicon nanoparticles and contended that this addition diminished the eutectic structure's size and promoted a uniform distribution in the bonding area.²⁴ Shen et al. added ZrO₂ nanoparticles into an Sn-Ag filler and showed that this addition controlled the formation of intermetallic particles during solidification.²⁵

Elements that greatly affect gamma strengthening are high melting point elements, such as molybdenum, tungsten, tantalum, and niobium.^{26,27} Molybdenum and tungsten have large atomic sizes for solid solution strengtheners and therefore reduce diffusion at elevated temperatures.²⁶ There are only two elements that raise the solidus temperature in nickel alloys, i.e. cobalt and tungsten.²⁶ Based on the binary phase diagrams, at > 900°C, there is significant solubility between Ni, W, and Cr. It can be concluded that Ni and W elements are prone to form a solid solution during the brazing thermal cycle. It is expected that the mutual diffusional activity between Ni and W will strengthen the interface region. On the other hand, there is a growing consensus that the wetting of the base metal faying surfaces by the interlayer and the mutual reactivity play a vital role in the brazing process.^{2,11–15} Hence, proper wetting and low reactivity are desirable issues in brazing processes. The approach of adding nanosized ceramic particles into the filler which has been proposed in the available literature was not successful in providing proper wetting. Regardless of the heating temperature and its effects on viscosity, adding metallic elements like

W and Co into the brazing filler metal can improve wetting. Therefore, tungsten, owing to its aforementioned excellent properties, has become a promising candidate for improving joint properties. However, it is noteworthy that excessive amounts of chromium, molybdenum, tungsten, and rhenium promote the formation of topological closed-packed (TCP) phases, such as μ , σ , δ , etc. TCP phases are not FCC crystal structures; in fact, the μ phase has a rhombohedral cell and the σ phase a tetragonal cell. Although molybdenum, tungsten, and chromium increase the strength and corrosion resistance of the γ phase, too much will result in the formation of deleterious TCP phases, which are highly brittle.²⁸ Finally, the addition of refractory elements such as W to the filler can effectively improve the high-temperature performance of NIMONIC 105 superalloy brazements.

In this work, two fillers, BNi-2 and W-rich BNi-10, were used to join the NIMONIC105 superalloy via brazing. The effects of tungsten addition on the metallurgical properties of the joints were investigated. The formation of intermetallic and eutectic phases was studied by back-scattered electron (BSE) image, energy dispersive X-ray spectroscopy (EDS), EDS mapping, and X-ray diffraction (XRD), as well as hardness testing. The innovative aspect of this study is surveying the influence of the tungsten addition to the filler on the microstructural features, hardness, strength, and fracture surface characteristics of the brazements. It is hoped that this novel approach will help to arrive at a convenient solution to the problem of joining superalloys.

EXPERIMENTAL

NIMONIC 105 superalloy and commercially obtained BNi-2 and BNi-10 fillers were received as the experimental materials in this study. According to ASM International, BNi-2 filler is an appropriate brazing filler metal for high-temperature, high-stress moving engine components and heavy, non-moving structures (variable gaps), and is appropriate for jet engine diffuser components.² The compositions of the base metal and the two fillers were analyzed experimentally, and the results are given in Table I. The fillers contained boron and silicon as MPDs. Two specimens were prepared by cutting for metallography and shear strength testing with the dimensions of 20 mm × 20 mm × 2.5 mm and 40 mm × 20 mm × 2.5 mm, respectively. The specimens were ultrasonically cleaned in an acetone bath to remove adhered contaminants and then dried in air. For preparing the shear strength test specimens, the samples were cut into dimensions of 40 mm × 20 mm × 2.5 mm. Then, the filler in the form of a paste with a thickness of 1 mm was applied to join the NIMONIC 105 superalloy. Solidus and liquidus temperatures of the BNi-2 brazing filler were 970°C and 1000°C, respectively, while solidus and liquidus temperatures of the BNi-10 brazing filler were 970°C

Table I. Chemical compositions of Nimonic 105 superalloy and BNi-2 and BNi-10 fillers (at.%)

	Ni	Co	Cr	Mo	Al	Si	Fe	Ti	Cu	B	W
NIMONIC105 superalloy	Bal.	18.41	14.93	5.01	4.64	0.11	1.0	1.37	0.2	–	–
BNi-2 filler	Bal.	–	7.0	–	–	4.5	3.0	–	–	3.0	–
BNi-10 filler	Bal.	–	12.0	–	–	3.5	3.5	–	–	2.5	16.0

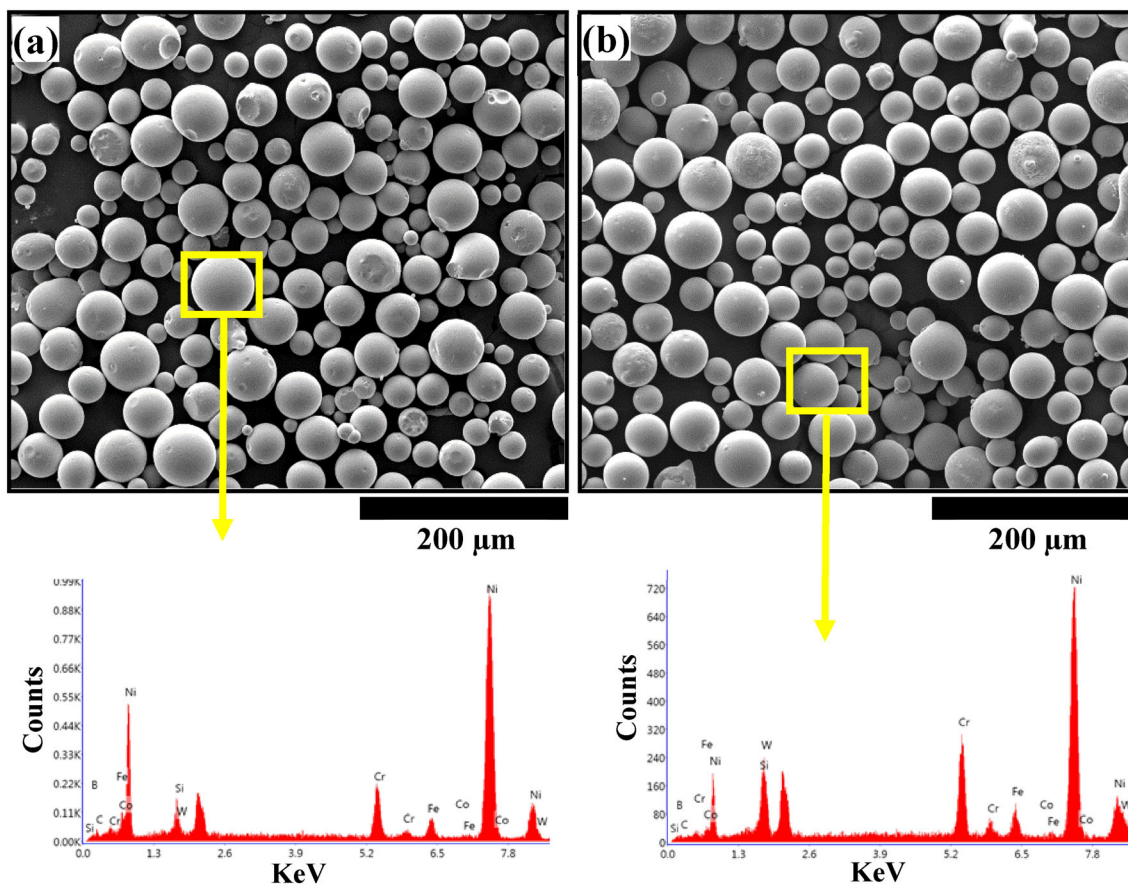


Fig. 1. Secondary electron (SE) images showing the morphology of the fillers accompanied by the EDS spectrum correspond to (a) BNi-2 and (b) BNi-10 fillers.

and 1105°C, respectively, so the brazing temperature was selected at a temperature above 970°C. The morphologies of the fillers accompanied by the EDS spectra are shown in Fig. 1. Note the W peak in the EDS spectrum of the BNi-10 filler (Fig. 1b). Experiments were performed in an electrical furnace with a vacuum of 1×10^{-4} Pa. The sample assembly was first heated to 750°C and held for 30 min. Then, the temperature was increased to 950°C and held for 30 min. Finally, the temperature was increased to a specified brazing temperature (1200°C). The optimized holding time was 7 min.

Following the brazing process, transverse cross-sections were prepared for microstructural observations with an optical microscope and scanning

electron microscope (SEM; TESCAN MIRA3). The etchant was composed of a solution of 15 mL HCl, 10 mL HNO₃, 10 mL acetic acid, and 5 mL glycerol. The etching time was 5 s. The SEM (TESCAN MIRA3) was equipped with an EDS analysis system and employed to analyze the chemical composition of the present phases at the interface. For the microhardness test, a WOLPERT machine was used that was able to measure microhardness at micro-scale with a 50gf load weight according to ASTM standard E384 (2017). The indenter was a diamond-based pyramid. The room-temperature shear strength of the joints was measured by a tensile test machine (INSTRON-5500R) according to ASTM standard D1002-99²⁹ at a crosshead speed of 1 mm/

min. The characterization of the precipitates and intermetallic phases in the fracture surface was preformed using XRD (Philips PW1730).

RESULTS AND DISCUSSION

Microstructural Characterization of the Joints

Figure 2 shows weld maps from samples bonded using BNi-2 (Fig. 2a) and BNi-10 (Fig. 2b) as filler. As seen in Fig. 2, no obvious cracks can be observed in the joint zones. This observation confirms the appropriate wettability of the fillers that, in turn, resulted in good metallurgical bonding in the brazements. EDS mapping analyses were also conducted to investigate the distribution of Ni, Cr, Si, and W to distinguish the boundaries of the dissolution and the widening layers in the joints, as shown in Fig. 2. The boundary of each layer can be clearly distinguished regarding its elemental distribution. The EDS map corresponding to Cr shows that

chromium-rich precipitates are formed in the joint region. According to the literature,^{8,30} these precipitates are chromium boride, which reduce the chromium content in the brazement and would have a detrimental effect on the high-temperature performance of the joint and decrease its corrosion resistance. It is evident from Fig 2 that the chromium distribution in the joint region of the brazement in the case of using BNi-10 as a filler (Fig. 2b) is much more uniform in comparison with the specimen brazed using BNi-2 as a filler (Fig. 2a). This is due to the high W content of the BNi-10 filler (~ 16 at.%). In the initial heating process, the diffusion mechanism of W with a high melting point is not activated, whereas Cr and Ni, which have low melting points, begin to mutually diffuse, as shown in Fig. 2. Therefore, tungsten addition was effective in retarding diffusion of solute atoms, thus hindering the precipitation of borides. Therefore, as the EDS map corresponding to Si shows (Fig. 2a), when the filler is lacking in W, a large number of Si atoms

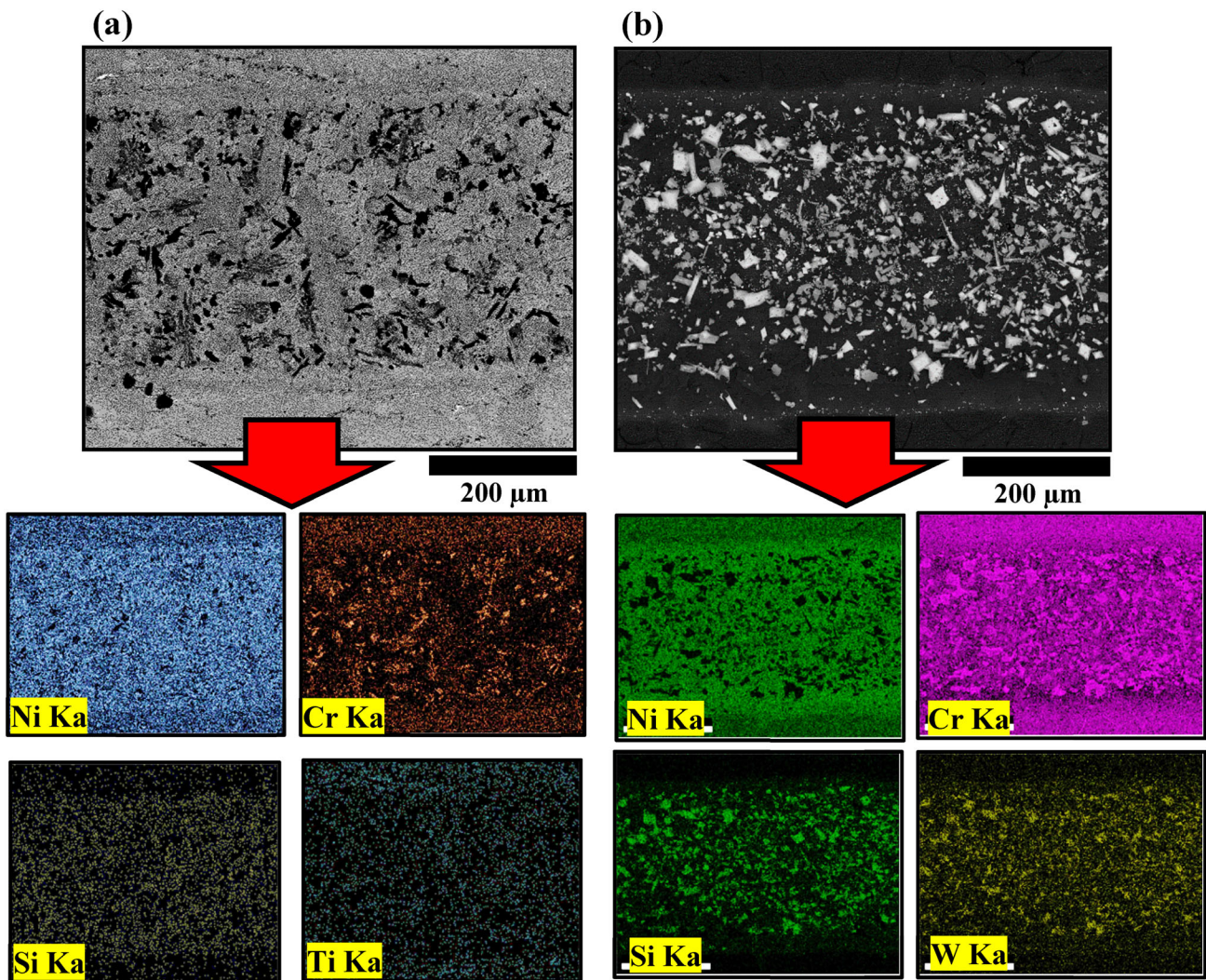


Fig. 2. Low-magnification back-scattered electron (BSE) images showing the overall microstructure of the bond and corresponding EDS mapping analyses of brazed samples using (a) BNi-2 and (b) BNi-10 as fillers

can diffuse and traverse the interlayer, leading to significant Si content at the two ends of the joint region (far from the filler). On the other hand, the EDS map corresponding to Si (Fig. 2b) shows the presence of W in the filler can effectively control the diffusion of Si and acts as a diffusion barrier. Hawk²⁸ reported the formation of WSi_2 precipitates when using BNi-5 braze alloys, which is in good accordance with this study. Another interesting matter shown in Fig. 2a is the distribution of Ti across the joint. Titanium is an alloying element in the NIMONIC105 base and is not present in the chemical composition of the BNi-2 filler. However, there is a significant distribution of this element in the joint region. This is in accordance with the study of Xu et al.,³¹ who concluded that Ti was likely to increase the dissolution of the filler to the base materials.

The interface micrographs of the specimens brazed using BNi-2 (Fig. 3a) and BNi-10 (Fig. 3b) as filler are shown in as BSE images. There are four individual microstructural zones:

- NIMONIC105 base metal
- Diffusion-affected zone (DAZ)
- Isothermally-solidified zone (ISZ)
- Athermally-solidified zone (ASZ)

Discrete second-phase particles with two blocky and acicular morphologies distributed in the γ -matrix can be seen in the microstructure of the base metal region immediately adjacent to the isothermally-solidified region (Fig. 3a). It is apparent from Fig. 3a that the morphology of these precipitates changes from globular to needle-like, as they get away from the interface. This is in accordance with the study of Li and Liu,^{6,7} who reported that the morphology of these secondary phases depends on shrinkage stresses arising from isothermal solidification. In the vicinity of the NIMONIC/filler interface, more shrinkage stresses developed. As a result, precipitates become spherical adjacent to this interface and acicular beyond it.

EDS chemical analysis of acicular and blocky DAZ precipitates is shown in Fig. 4a and b, respectively. As anticipated, and in accordance with the literature,^{5,9} all secondary phases contained significant boron, although the standard-less EDS used could not give an accurate measure of the actual boron percentages. Based on the compositional analysis, both acicular and cuboidal precipitates in DAZ contain higher chromium content in comparison with γ BNi-2 filler. On the other hand, boron solubility in nickel is very low (0.3 at.% in the temperature range of 1060–1120°C³²). As a result, when the concentration of boron exceeds the solubility limit in the base metal, secondary precipitates can form. Boron combines with chromium or molybdenum to form chromium borides within the gamma-grain boundaries. The precipitates in the DAZ were mainly composed of brittle Ni-Cr-Mo-rich borides. This is in agreement with the results of Wu et al.⁹ During the brazing process, silicon and boron atoms diffused to the base metal from the molten filler. Here (in DAZ), boron reacted with elements from the base metal to form Ni-Cr-Mo-rich borides. Formation of these Ni-Cr-Mo-rich particles in DAZ is undesirable from the mechanical properties and corrosion resistance points of view. Firstly, the creation of these brittle and hard IMCs will destroy the strength of the joint. It is believed that initial cracks available in the IMC layers subsequently propagate during shear testing.²³ Secondly, the formation of the chromium boride precipitates is responsible for localized depletion in the concentration of Cr and some other refractory elements, such as Mo in the DAZ. Figure 3b indicates that the presence of W in the filler (BNi-10) can effectively modify the boride formation. Introducing W to the filler has the effect of reducing the boride sizes. Furthermore, the W content will play a role in breaking the continuous nature of the borides. It is apparent from Fig. 3b that the resulting borides are not only much smaller but also sparsely distributed.

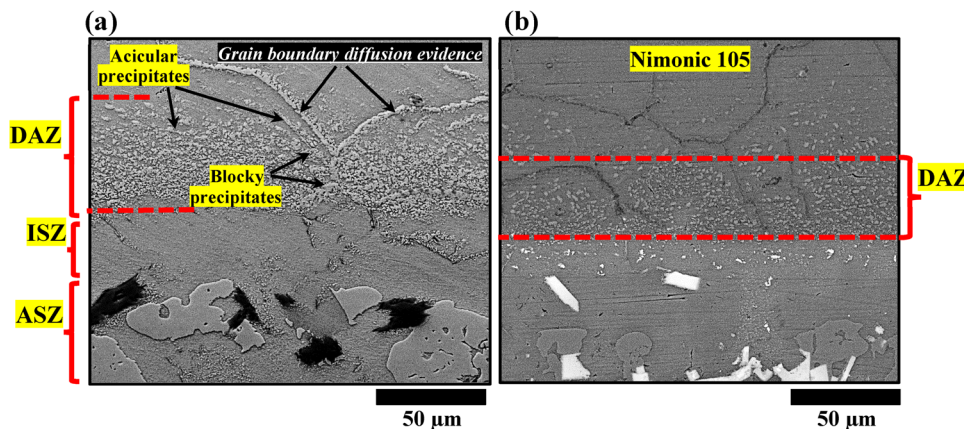


Fig. 3. Magnified images of the DAZ in Fig. 2 for NIMONIC105 superalloy joints brazed at 1200°C using (a) BNi-2 and (b) BNi-10 as fillers

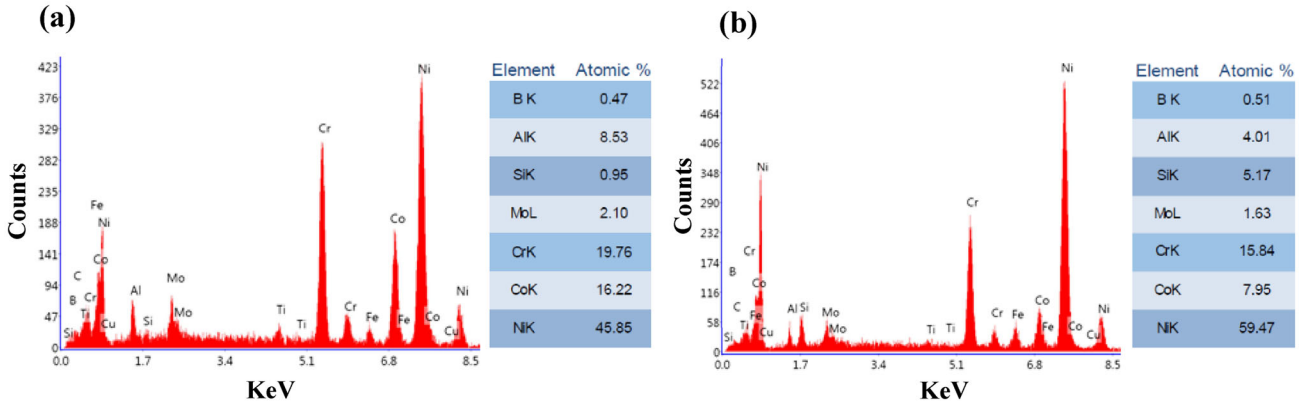


Fig. 4. EDS spectra, accompanied by the chemical composition of (a) acicular and (b) blocky DAZ precipitates shown in Fig. 3a

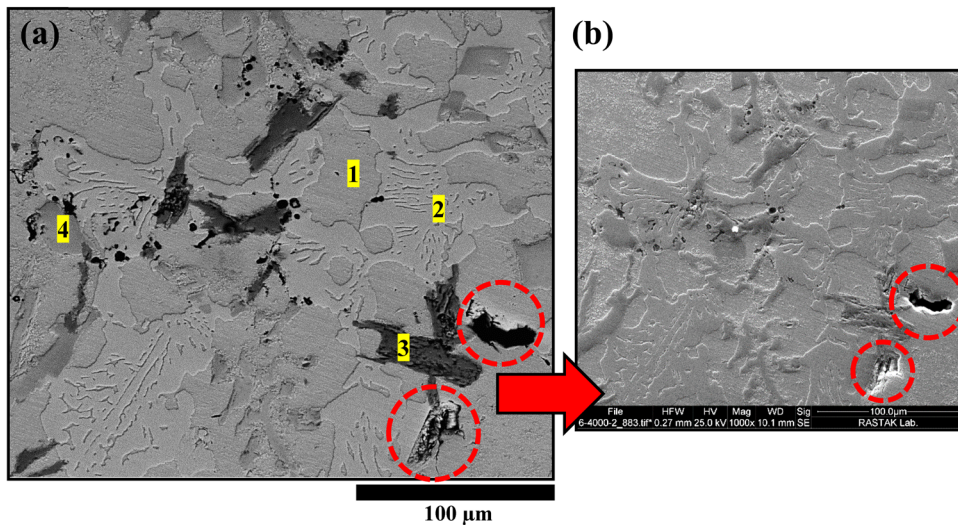


Fig. 5. (a) BSE and (b) SE micrographs of the joint center for the sample brazed using BNi-2 as filler

Table II. EDS analysis (at.%) of selected regions shown in Fig. 5

Region	Ni	Co	Cr	Mo	Al	Si	Fe	Ti	B	Possible phases
1	69.20	6.21	8.24	0.14	5.43	6.13	3.17	0.59	0.28	Gamma solid solution
2	75.21	7.19	5.14	0.09	5.58	0.72	2.13	1.69	1.45	Ni-rich boride
3	2.64	0.81	84.48	6.18	1.07	0.94	1.17	0.59	0.19	Cr-rich IMC
4	68.32	6.47	4.86	0.12	3.87	1.11	1.87	2.26	7.08	Ni-rich boride

BSE micrographs of the joint center corresponds to the sample brazed with BNi-2 as filler are shown in Fig. 5. The EDS technique was used to identify each phase individually. Regions in a joint created using BNi-2 as the filler have been analyzed using EDS at some selected regions, marked as 1, 2, 3, and 4 in Fig. 5. The concentration of Ni, Co, Cr, Mo, Al, Si, Fe, Ti, and B in the regions analyzed by EDS are listed in Table II. The formation of the eutectic that contains fine precipitates is visible in the figure, and the presence of some eutectic islands and intermetallics at the centerline of the joint suggests that

the isothermal solidification of the liquid phase was not completed in this specimen. According to the literature,^{8,22,23} if complete isothermal solidification takes place during the brazing process of Ni-based superalloys, the microstructure will contain substantially a gamma nickel solid solution and some particles of borides, silicides, or carbo-borides dispersed in the gamma Ni phase. These particles are formed due to the low solubility of boron in nickel (0.3 at.%³²) during brazing or cooling due to the saturation of MPDs. However, in practice, complete isothermal solidification does not occur. Therefore,

as shown in Fig. 5, the resulting microstructure often contains brittle phases, such as Ni-rich boride and Cr-rich IMCs, besides gamma solid solution. When a Ni-B-Cr ternary braze alloy (e.g. BNi-2) is used a primary γ -Ni solid solution and several types of eutectic constituents formed through binary and ternary invariant eutectic reactions of $L \rightarrow \gamma + \text{Ni}_3\text{B}$ at 1042°C and $L \rightarrow \gamma \text{ FCC} + \text{Ni}_3\text{B} + \text{CrB}$ at 997°C will be found in the microstructure.²² Table II indicates that the joint center in Fig. 3 contains the matrix solid solution of gamma-nickel (region 1 in Fig. 5), Ni-rich borides (regions 2, 4), and Cr-rich phases (region 3). Gamma solid solution (region 1) is the first phase that forms and grows during cooling. Since there is a large amount of silicon (6.13 at.%), the phase that forms with the other elements in the solid solution is the most likely $\text{Ni}_3(\text{Si}, \text{B})$. The ongoing formation of gamma nickel leads to the rejection of alloying elements such as Cr, Mo, Al, and B to liquid.³³ As a result, the remaining liquid becomes enriched by these elements. Regions 3 and 4 in Fig. 5, are Cr-rich intermetallics and Ni-rich borides, respectively. Arhami et al.⁵ have also reported the formation of the same phases in the ASZ of diffusion-brazed IN-939 using a Ni-Cr-B filler. These intermetallics would not be ideal phases to form because that would mean that chromium is being depleted from the matrix, thereby decreasing the corrosion resistance of the material. Further, the formation of this type of bulky brittle phases (borides or silicides) and network or eutectic phases around the solidified solid solution is detrimental to the mechanical properties of the brazed joint.

There are some void-like features observed in the BSE micrograph that formed within the joint in ASZ adjacent to bulky brittle and eutectic phases. The void-like features are marked in Fig. 5a. In order to determine whether or not these features are real voids, a secondary electron (SE) micrograph of the same zone was taken and is shown in Fig. 5b. It is apparent from the SE image that electron-number effects make the edges of surface voids brighter than the rest of the surface. It can be concluded that Fig. 5 shows many voids in the ASZ, indicating a brittle braze owing to intermetallics. This agrees with the results of Kim et al.³⁴ The voids formed due to solidification shrinkage in the ASZ can reduce the strength.

The microstructure and elemental distributions of the brazed sample in the case of using BNi-10 as the filler are shown in Fig. 6. The EDS maps in Fig. 6b and c indicate that all the secondary phases are lean in Ni and Fe while containing significantly higher Cr, Si, Mo, and W contents (Fig. 6d, e, f, and g). This observation is in accordance with the study of Huang et al.,²² who investigated the effect of tungsten addition on the nucleation of borides in wide-gap brazed joints. They suggested that tungsten, chromium, and molybdenum partitioned preferentially to silicides and borides, either as nucleation sites as unmelted tungsten particles,

for boride nucleation, or by creating tungsten borides during the brazing process. The EDS concentration analysis results corresponding to the selected regions marked as 1, 2, 3, and 4 in Fig. 6a are listed in Table III. Figure 6a shows that the continuous nature of the bulky brittle and network eutectic phases observed in the brazed sample in the case of using BNi-2 as a filler (Fig. 5) is no longer an issue. It seems that the presence of W in the BNi-10 filler has effectively contributed to the boride nucleation via supplying additional nucleation sites, and has the potential to reduce the size and continuous nature of the undesirable phases. Figure 7 illustrates the five critical steps involved in isothermal solidification of this specimen:

- 1- Once the brazing temperature is reached, the filler liquefies completely and surrounds the refractory W-rich particle, which retains its solid state and original shape. Region 1 in Fig. 6a represents one of such W-rich particles, and Table III shows its chemical composition. The MPD concentration is unchanged in this stage.
- 2- MPD diffuses from the liquid into the W-rich particles. The driving force of this diffusion is the concentration gradient at the liquid/W-rich particle interface. Over the brazing time, compositional gradient commences developing in the W-rich particles. As the solubility of the MPD in the W-rich particles is limited, sparse IMCs commence forming in them.
- 3- When the MPD concentration at the interface of the W-rich particles reaches C_S , continuity of diffusion will be accompanied by dissolution of the particles' surface. Recession or erosion of the W-rich particles is obvious in Fig. 6a. The erosion of the W-rich particles continues until the liquid reaches C_L . Here, the maximum volume of liquid in the brazing cycle will form.
- 4- MPD diffusion into W-rich particles continues due to the driving force of the compositional gradient. The consequence of the continuous discharge of MPD from the liquid is a reduction in the amount of liquid, i.e. commencing of isothermal solidification. Region 2 in Fig. 6a is a typical product of the aforementioned isothermal solidification. According to Table - III, the main constituent of this region is nickel (72.93 at.%), which suggests that the matrix is gamma-nickel with solid solution strengthening elements of chromium (8.74 at.%), cobalt (4.06 at.%), and silicon (5.15 at.%). The solid formed at the interface due to diffusion assumes a composition of C_S . The continuity of diffusion of MPD in the W-rich particles increases the solid volume (region 1 in Fig. 6a) and the MPD concentration in the W-rich particles (5.43 at.% Si).
- 5- Isothermal solidification will continue until the last remaining liquid transforms into a

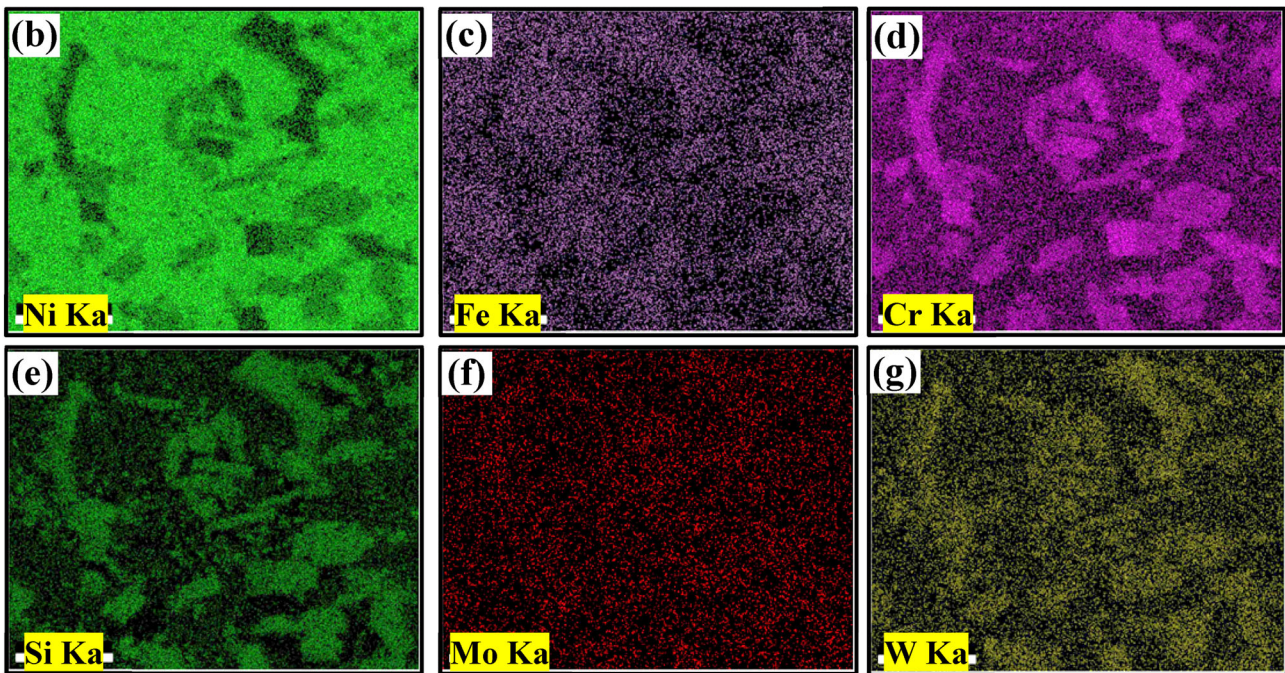
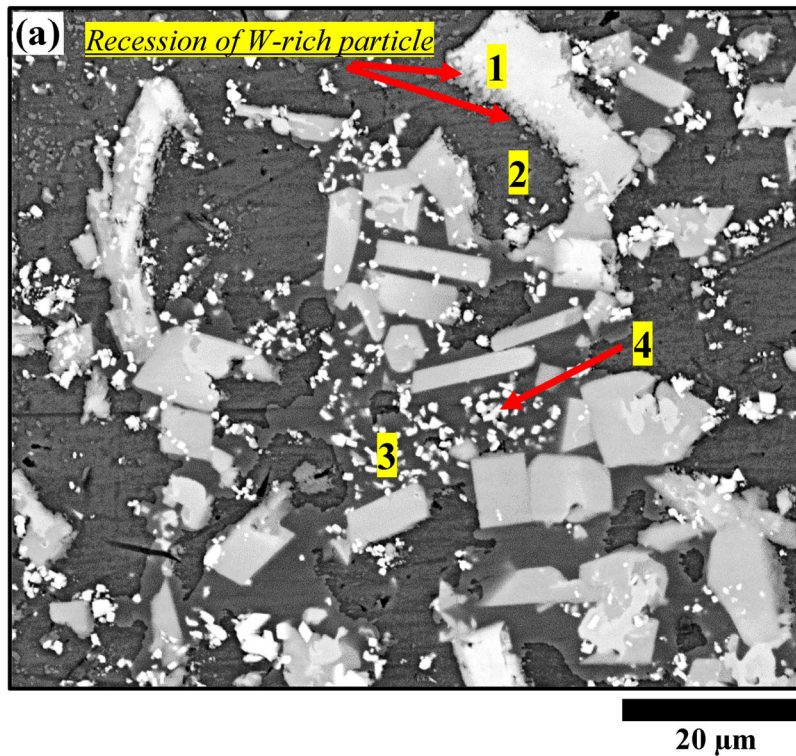


Fig. 6. (a) BSE micrograph of the joint center for the sample brazed using BNi-10 as filler and corresponding EDS maps, showing concentrations for (b) Ni, (c) Fe, (d) Cr, (e) Si, (f) Mo, and (g) W

gamma-nickel solid solution. Region 3 in Fig. 6a is a typical product of the aforementioned fulfillment of complete isothermal solidification. According to Table III, the main constituent of this region is also nickel (79.66 at.%), which suggests that the matrix is gamma-nickel with solid solution strengthening elements of chromium (5.54 at.%), cobalt

(4.12 at.%), and silicon (1.21 at.%). However, a large concentration gradient of MPD exists in the W-rich particles. According to Table III, the silicon content of the W-rich particles (region 1 in Fig. 6a) is as high as 5.43 at.%. During cooling from the brazing temperature, fine precipitates (such as in region 4 in Fig. 6a) will form depending on the solubility of the

Table III. EDS analysis (at.%) of selected regions shown in Fig. 6

Region	Ni	Co	Cr	Mo	Al	Si	Fe	Ti	W	Possible phases
1	10.56	3.07	43.62	3.17	0.92	5.43	4.22	1.51	27.51	W-rich particle
2	72.93	4.06	8.74	0.44	2.46	5.15	4.42	0.64	1.41	γ -nickel solid solution
3	79.66	4.12	5.54	0.55	3.72	1.21	2.99	1.36	0.87	γ -nickel solid solution
4	46.60	3.89	11.52	2.43	1.70	4.94	2.58	1.37	24.97	NiW and Ni ₄ W IMCs

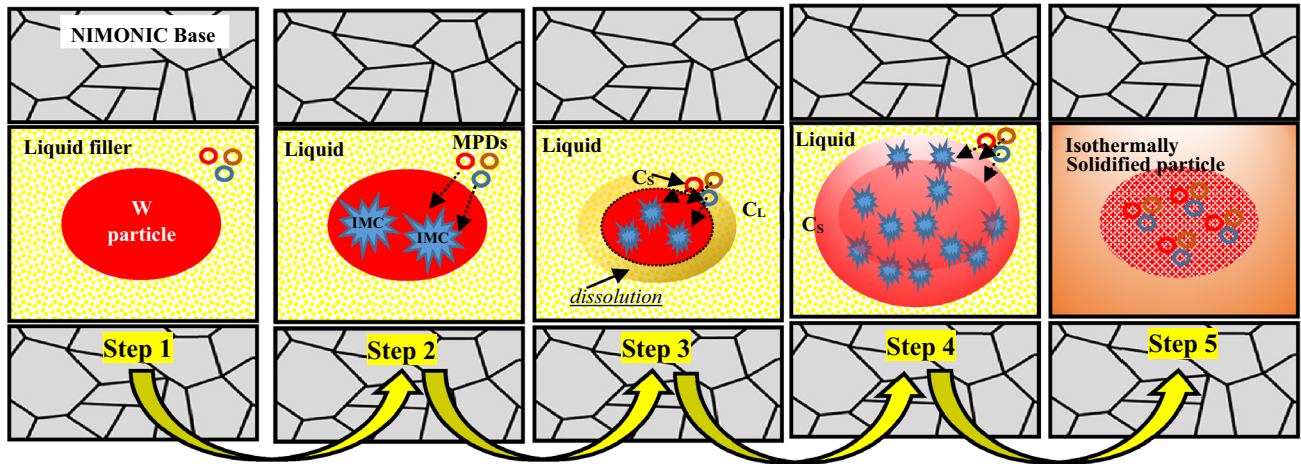


Fig. 7. The isothermal solidification process in Fig. 6

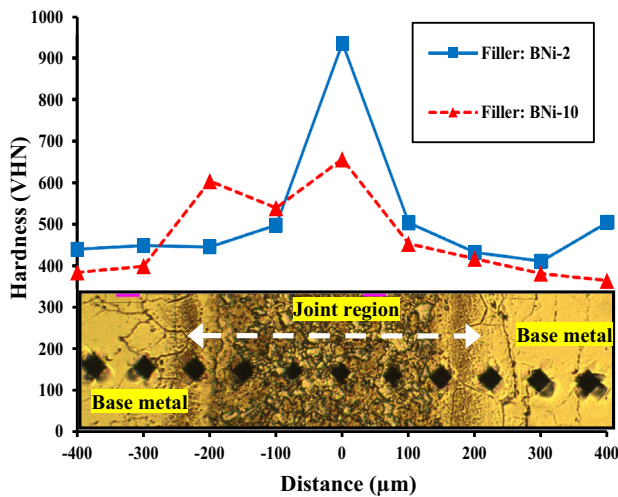


Fig. 8. Microhardness profiles across the joint region as a function of distance from the center of the interface for joints created using BNi-2 and BNi-10 as fillers

different elements. From Table III, it can be found that the nickel content in these fine particles (region 4) was higher (46.6 at.%), followed by tungsten (24.97 at.%) and chromium (11.52 at.%). According to a recent phase diagram in the binary Ni-W system,³⁵ Ni₄W, NiW and NiW₂ are the stable IMCs at $T = 1173$ K. Unlike the bulky brittle phases (borides or silicides) and network or eutectic phases found in the specimen brazed using

BNi-2 as a filler (Fig. 5), these fine precipitates have minimal impact on the properties of the joint.

Mechanical Properties of the Joints

Microhardness

Microhardness profiles of the bonds made using BNi-2 or BNi-10 as filler combined with microstructure are illustrated in Fig. 8. A high hardness value (935 VHN) is observed in the joint region of the specimen brazed using BNi-2 as the filler. These values are much greater than those for the NIMONIC105 base metal. Khakian et al.⁸ have reported that intermetallic phases that form during non-isothermal solidification possess very high hardness (750 HVN). These brittle phases are suitable sites for crack initiation and therefore reduce the strength of the joint. These high hardness values are not observed in the joint region of the specimen brazed using BNi-10 as the filler. This confirms that adding tungsten to the filler metal leads to a more homogenous interface region via controlling the diffusion of MPD that, in turn, can effectively modify the boride formation. As mentioned, W content will play a role in breaking the continuous nature of the borides. Figure 8 indicates that using BNi-10 filler resulted in more uniform hardness profiles across the joint that, in turn, led to less stress concentration. Remarkably, the hardness between 450 and 550 HVN tended to correspond

with indents on the eutectic constituent and matrix. The high hardness of about 900 HVN suggests the probability for the precipitation of bulky IMCs discussed in Fig. 5. Therefore, the microstructure and microhardness are consistent with the formation of brittle IMCs in the joint region of specimens brazed using BNi-2 as the filler. To minimize the extent of these detrimental phases, introducing W to the filler is a successful approach. The addition of W to the filler, as a diffusion barrier, has the effect of reducing boride sizes via controlling the diffusion of MPDs. Further, W content will play a role in breaking the continuous nature of the borides and undesirable continuous eutectic phases.

Shear Strength

Room-temperature shear strength test results of the bonds made using BNi-2 or BNi-10 as the filler are illustrated in Fig. 9. The strengthening effect of tungsten is obvious. The shear strength of the brazed joints increased significantly from 81.8 MPa to 88.1 MPa with the addition of tungsten. This can be attributed to the voids observed in Fig. 5. Voids are significant stress concentration sites and have a detrimental influence on the mechanical properties of the joints. The ductility of the specimen brazed with BNi-10 as the filler was as high as 17.1%, which is approximately 68% of the ductility of NIMONIC 105. The maximum ductility recorded in the present study is higher than those obtained in all similar previous works with different variables.^{5–8,31,34} Liu et al.²³ stated that the ductility of the brazed joints depends primarily on the quantity of the boride precipitation in the DAZ. As shown in Fig. 3, the presence of W in the filler (BNi-10) can effectively modify the boride formation. Introducing W to the filler has the effect of reducing boride sizes. It is apparent from Fig. 3b that the resulting borides are not only much smaller but also sparsely distributed. In other words, the addition of W to the filler, as a diffusion barrier, has the effect of reducing boride sizes via controlling the diffusion

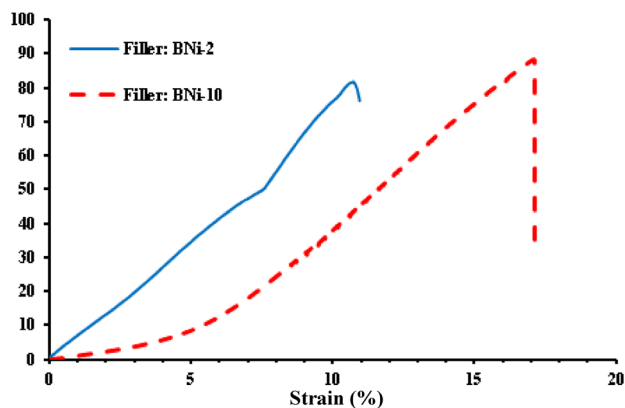


Fig. 9. Stress–strain curves obtained by a room-temperature shear strength test of the brazed joints with respect to the two different brazing fillers discussed in this study

of MPDs. During brazing, more boron and silicon diffused out of the filler metal and into the additive powder, which decreased the amount of eutectic. Another mechanism that improved shear strength is the diffusion of the solid-solution strengthening elements, such as chromium, tungsten, aluminum, and titanium that diffused from the additive powder into the filler metal powder.

Fractography The SEM micrographs were obtained from brazement fractured surfaces and the fractographs with the composition of the filler are shown in Fig. 10. As seen in Fig. 10a in the sample, brazed using BNi-2 as filler, failure occurred across the bonded interface because this area includes bulky brittle Ni-rich borides and Cr-rich phases besides network or eutectic phases around the solidified solid solution. The SEM micrograph corresponding to the fracture surface of this specimen shows faceted features that indicate fiddling amounts of plastic deformation and brittle fracture mode. In the sample brazed using BNi-10 as the filler, failure occurred at the DAZ of the bonded interface (Fig. 10b), indicating that the shear strength of this joint was relatively higher. Comparatively, when tungsten was added to the filler, some ductile dimples were observed in the fracture surface, showing a more ductile fracture. The SEM micrograph corresponding to the fracture surface of this specimen shows micro-void coalescence in between larger ridges of deformed material. Therefore, Fig. 10b shows the mixed failure showing brittle and ductile fracture modes simultaneously in the SEM fractograph when using BNi-10 as filler.

Identifying Intermetallic Compounds

An XRD analysis was conducted to characterize the precipitates and intermetallic phases in the joint region. The XRD patterns corresponding to the fracture surfaces of the brazements of both samples including the BNi-2 and W-rich BNi-10 fillers are shown in Fig. 11. The XRD pattern obtained from the fracture surface confirms the creation of different borides and silicides such as SiCr_3 , Ni_2B , Cr_2B , and NiSi , in addition to IMCs such as FeNi , during the brazing process in the joint area made using BNi-2 as an interlayer (Fig. 11a). This is in good agreement with microstructural observations indicating the formation of Ni-Cr-Mo -rich particles in the DAZ. On the other hand, Fig. 11b shows that, by introducing W into the filler, the variety of precipitates formed in the interface region is reduced. The XRD pattern corresponding to the brazement made via W-rich BNi-10 as the filler (Fig. 11b) shows that peaks for W are detected on the fracture surface of the specimen. The recognized second phases in the interface of this specimen are CrSi_2 , Cr_2B , and FeNi . Comparison of the XRD patterns in Fig. 11 suggests that tungsten addition to the filler effectively retarded MPD atom diffusion, so that the

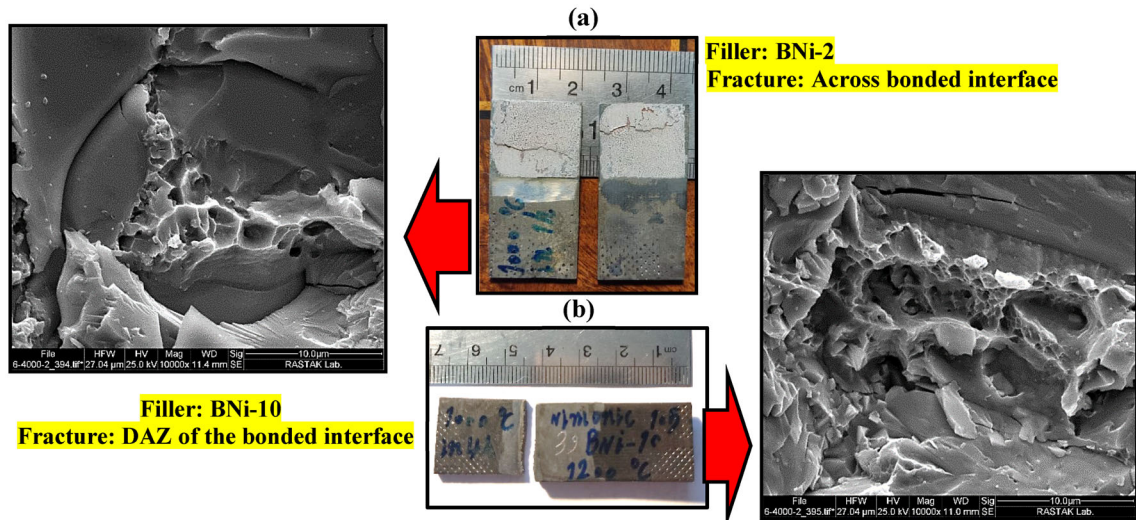


Fig. 10. Fracture zone and SEM fractographs of the surfaces of shear strength specimens corresponding to joints brazed with (a) BNi-2 and (b) BNi-10 as fillers

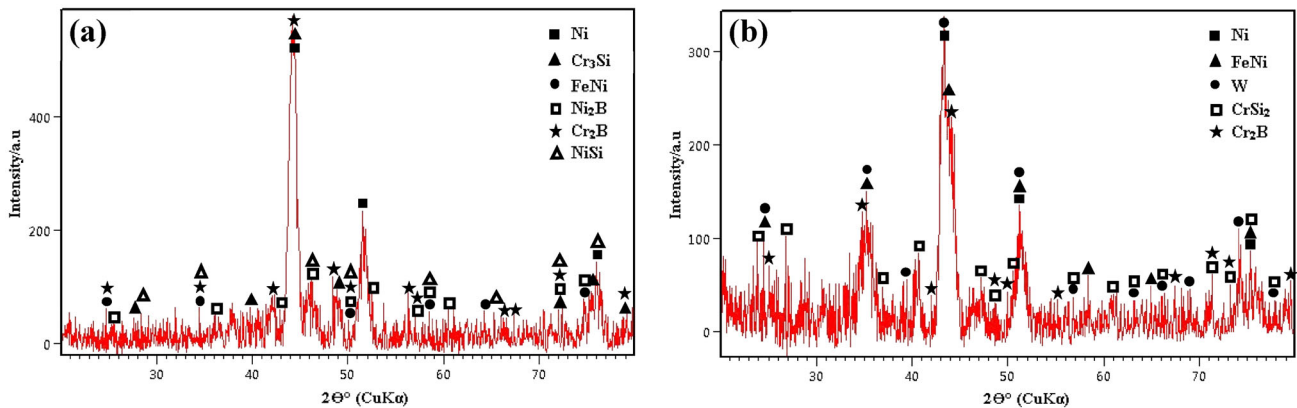


Fig. 11. X-ray diffraction patterns of the fracture surface of brazements made via (a) BNi-2 and (b) W-rich BNi-10 as fillers

precipitation of undesirable Ni_2B and NiSi is hindered in the case of using BNi-10. Additionally, the XRD results indicate that, at the interface of the brazement made via BNi-10, CrSi_2 has formed instead of Cr-rich Cr_3Si silicide. Since the formation of Cr-rich silicides would mean chromium depletion from the matrix, decreasing the corrosion resistance of the material CrSi_2 is preferred. The XRD results are also in line with the shear strength test results. Since the ductility of the brazed joints depends primarily on the quantity of the boride precipitation in DAZ, lack of Ni_2B and NiSi formation resulted in the high ductility of 17.1% in the specimen brazed via BNi-10 when compared with 10.95% for the specimen brazed via BNi-2.

CONCLUSION

1. The precipitates in the DAZ were mainly composed of brittle Ni-Cr-Mo-rich borides. The

formation of these Ni-Cr-Mo-rich particles in the DAZ is undesirable from the mechanical properties and corrosion resistance points of view. Tungsten addition to the filler was effective in retarding MPD atom diffusion, thus hindering the precipitation of these borides.

2. The joint center in the specimen brazed using BNi-2 as the filler contains the matrix solid solution of gamma-nickel, bulky brittle Ni-rich borides, and Cr-rich phases. The formation of this type of phase (SiCr_3 , Ni_2B , Cr_2B , and NiSi) and network or eutectic phases around the solidified solid solution is not only detrimental to the mechanical properties of the brazed joint but also degrades the corrosion resistance of the joint.
3. The presence of W in the BNi-10 filler has effectively contributed to the boride nucleation via supplying additional nucleation sites, and has the potential to reduce the size and continuous nature of the undesirable phases. Unlike

the bulky brittle phases (such as SiCr_3 , Ni_2B , Cr_2B , and NiSi) and network or eutectic phases found in the specimen brazed using BNi-2 as the filler, the W-rich filler (BNi-10) created fine precipitates (CrSi_2 , Cr_2B) that have minimal impact on the properties of the joint.

- Using the BNi-10 filler resulted in more uniform hardness profiles across the joint. A fairly high hardness value of 935 VHN, observed in the joint region of the specimen brazed using BNi-2 as the filler is relevant to intermetallic phases that form during the non-isothermal solidification process. These high hardness values are not observed in the joint region of the specimen brazed using BNi-10 as the filler.
- The shear strength of the brazed joints increased significantly from 81.8 MPa to 88.1 MPa with the addition of tungsten. The lack of Ni_2B and NiSi formation resulted in a high ductility of 17.1% in the specimen brazed via BNi-10 when compared with 10.95% for the specimen brazed via BNi-2.
- To minimize the extent of detrimental phases, introducing W to the filler is a successful approach. When tungsten was added to the filler, some ductile dimples were observed on the fracture surface, showing a more ductile fracture. The addition of W to the filler, as a diffusion barrier, has the effect of reducing boride sizes via controlling the diffusion of MPDs. Furthermore, W content will play a role in breaking the continuous nature of the borides and undesirable continuous eutectic phases.

PROPOSAL FOR FUTURE WORK

The quality of the brazement needs to be improved by the further design of interlayer composition and further application of post-braze heat treatment. This will include the insertion of an interlayer containing a high amount of refractory elements such as cobalt and tungsten that effectively retard atomic diffusion and control the formation of brittle boride precipitates. The authors intend to study this approach in subsequent studies.

CONFLICT OF INTEREST

The authors declare that they have no conflict of interest.

REFERENCES

- Y. Zhua, Z. Zhua, Z. Xianga, Z. Yinb, Z. Wua, and W. Yana, *J. Alloys Compd.* 476, 341 <https://doi.org/10.1016/j.jallcom.2008.08.062> (2009).
- R. Barazandeh, M.A. Mofid, M. Jafarzadegan, and H. Nasiri Vatan, *Weld. World.* <https://doi.org/10.1007/s40194-022-01460-9> (2023).
- R.C. Reed, *The superalloys—fundamentals and applications* (Cambridge University Press, New York, 2006).
- M. Naalchian, M. Kasiri-Asgarani, M. Shamanian, R. Bakhtiari, and H.R. Bakhsheshi-Rad, *J. Mater. Res. Technol.* 13, 2144 <https://doi.org/10.1016/j.jmrt.2021.05.069> (2021).
- F. Arhami, S.E. Mirsalehi, and A. Sadeghian, *J. Mater. Process. Technol.* 265, 219 <https://doi.org/10.1016/j.jmatprotec.2018.10.021> (2019).
- W. Li, T. Jin, X. Sun, Y. Guo, H. Guan, and Z. Hu, *Scr. Mater.* 48(9), 1283 (2003).
- J. Liu, T. Jin, N. Zhao, Z. Wang, X.F. Sun, H.R. Guan, and Z.Q. Hu, *Mater. Sci. Forum* 546, 1245 (2007).
- M. Khakian, S. Nategh, and S. Mirdamadi, *J. Alloys Compd.* 653, 386 <https://doi.org/10.1016/j.jallcom.2015.09.044> (2015).
- N. Wu, Y.J. Li, and Q.S. Ma, *Mater. Des.* 53, 816 <https://doi.org/10.1016/j.matdes.2013.07.063> (2014).
- M.A. Mofid, and P. Lotfipoornasaji, *J. Met. Mater. Miner.* 31, 51 <https://doi.org/10.14456/jmmm.2021.7> (2021).
- M.A. Mofid, M. Farshbaf, and H. Naeimian, *Mater. Perform. Charact.* 10(1), 285 <https://doi.org/10.1520/MPC20200027> (2021).
- M.A. Mofid, and A. Mahdavi Nejad, *Mater. Chem. Phys.* 263, 124404 (2021).
- M.A. Mofid, H. Naeimian, M. Hajian Heidary, and M. Farshbaf, *J. Adv. Mater. Process.* 8(1), 55 (2020).
- H. Naeimian, and M.A. Mofid, *Trans. Nonferrous Met. Soc. China* 30, 1267 [https://doi.org/10.1016/S1003-6326\(20\)65294-3](https://doi.org/10.1016/S1003-6326(20)65294-3) (2020).
- H. Shakeri, and M.A. Mofid, *Met. Mater. Int.* 27, 4132 <https://doi.org/10.1007/s12540-020-00731-8> (2021).
- H. Naeimian, and M.A. Mofid, *Int. J. Mater. Res.* 111, 424 <https://doi.org/10.3139/146.111902> (2020).
- M.A. Mofid, and E. Loryaei, *Mater. Werkst.* 51, 413 (2020).
- M.A. Mofid, and E. Loryaei, *J. Mater. Res. Technol.* 8(5), 3872 (2019).
- D. McGuire, X. Huang, D. Nagy, and W. Chen, *J. Eng. Gas Turbines Power* 132, 062101 <https://doi.org/10.1115/1.4000136> (2010).
- M.A. Arafim, M. Medraj, D.P. Turner, and P. Bocher, *Mater. Chem. Phys.* 106(1), 109 (2007).
- J. Ruiz-Vargas, N. Siredey-Schwaller, N. Gey, P. Bocher, and A. Hazotte, *J. Mater. Process. Technol.* 213(1), 20 (2013).
- X. Huang, and W. Miglietti, *J. Eng. Gas Turbines Power* 13, 010801–010811 (2012).
- D. Liu, Y. Song, B. Shi, Q. Zhang, X. Song, H. Niu, and J. Feng, *J. Mater. Sci. Technol.* 34(10), 1843–1850 <https://doi.org/10.1016/j.jmst.2018.02.008> (2018).
- H.M. Hdz-García, A.I. Martínez, R. Muñoz-Arroyo, J.L. Acevedo-Dávila, F. García-Vázquez, and F.A. Reyes-Valdes, *Mater. Sci. Technol.* 30, 259 (2014).
- J. Shen, Y.C. Liu, Y.J. Han, Y.M. Tian, and H.X. Gao, *J. Electron. Mater.* 35, 1672 (2006).
- M. Durand-Charre, *The microstructure of superalloys* (CRC Press, 1997).
- C.T. Sims, *Superalloys* 1984, 399 (1984).
- C. Hawk, *Wide gap braze repairs of nickel superalloy gas turbine components*, (Colorado School of Mines, Golden, Colorado, 2016).
- ASTM standard D1002, Standard test method for apparent shear strength of single-lap-joint adhesively bonded metal specimens by tension loading (metal-to-metal) [S] (1999).
- O.A. Idowu, O.A. Ojo, and M.C. Chaturvedi, *Metall. Mater. Trans. A* 37A, 2787 (2006).
- Y. Xu, X. Qiu, S. Wang, C. Luo, Y. Lu, and F. Xing, *Vacuum* 184, 109793 (2021).
- ASM Handbook, *Alloy phase diagrams*, 10th edn. (ASM Handbook, 1992), pp. 283–292.

33. P. Sung, and D. Poirier, *Metall. Mater. Trans. A* 30(8), 2173 (1999).
34. Y.H. Kim, K.T. Kim, and I.H. Kim, *Key Eng. Mater.* 306–308, 935 (2006).
35. T.B. Massalski, H. Okamoto, P.R. Subramanian, and L. Kacprzak, *Binary alloy phase diagrams* (ASM International, 1990), p2883.

Springer Nature or its licensor (e.g. a society or other partner) holds exclusive rights to this article under a publishing agreement with the author(s) or other rightsholder(s); author self-archiving of the accepted manuscript version of this article is solely governed by the terms of such publishing agreement and applicable law.

Publisher's Note Springer Nature remains neutral with regard to jurisdictional claims in published maps and institutional affiliations.